

Thermal broadening of the Coulomb blockade peaks in quantum Hall interferometers

LACHEZAR S. GEORGIEV

Institute for Nuclear Research and Nuclear Energy, Bulgarian Academy of Sciences, 72 Tsarigradsko Chaussee, 1784 Sofia, Bulgaria, EU

PACS 11.25.Hf – Conformal field theory, algebraic structures
 PACS 71.10.Pm – Fermions in reduced dimensions (anyons, composite fermions, Luttinger liquid)
 PACS 73.43.-f – Quantum Hall effects

Abstract. - We demonstrate that the differential magnetic susceptibility of a fractional quantum Hall disk, representing a Coulomb island in a Fabry–Perot interferometer, is exactly proportional to the island’s conductance and its paramagnetic peaks are the equilibrium counterparts of the Coulomb blockade conductance peaks. Using as a thermodynamic potential the partition functions of the edge states’ effective conformal field theory we find the positions of the Coulomb blockade peaks, when the area of the island is varied, the modulations of the distance between them as well as the thermal decay and broadening of the peaks when temperature is increased. The finite-temperature estimates of the peak’s heights and widths could give important information about the experimental observability of the Coulomb blockade. In addition, the predicted peak asymmetry and displacement at finite temperature due to neutral multiplicities could serve to distinguish different fractional quantum Hall states with similar zero-temperature Coulomb blockade patterns.

[cond-mat.mes-hall] 8 Sep 2010

arXiv:1003.4871v3

The structure of the Coulomb blockade (CB) peaks in the conductance of a Fabry–Perot interferometer [1, 2], realized by two quantum point contacts (QPC) inside of a fractional quantum Hall (FQH) bar, operating in the strong-backscattering regime, depicted in Fig. 1, which is the stable fixed point of the renormalization group (RG) flow, has been widely investigated [3–5] because of its potential to unveil important intrinsic characteristics of the corresponding quasiparticle excitations. However, the zero-temperature CB patterns appeared to be unable to decisively distinguish FQH states with different topological order [6–8]. In this Letter we will demonstrate how the effective conformal field theory (CFT) for the FQH edges could be employed for the computation of the CB peaks’ parameters at non-zero temperature below the energy gap. We will show that the periodicity of the CB peaks could change with increasing the temperature T , and this could in principle be used to distinguish between different states with identical zero-temperature CB patterns [6].

We will be interested in the low-temperature, low-bias transport through the island, formed by the two pinched-off QPCs, see Fig. 1, when the leading conductance contribution comes from single-electron tunneling, known also

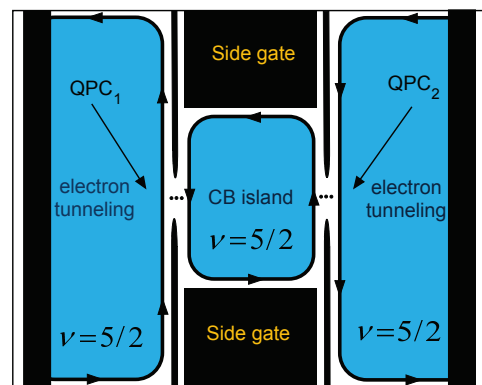


Fig. 1: (color online) Strong backscattering regime in Fabry–Perot interferometer. Two pinched-off QPCs inside of a $\nu = 5/2$ FQH bar create a CB island whose area, respectively magnetic flux, could be varied by changing the voltage of the side gates. Electrons could tunnel through the CB island only for special values of the flux for which single-electron spectrum of the island is degenerate.

as sequential tunneling, which is the dominant tunneling mechanism close to the center of the CB peaks at low temperature and bias [9]. Away from the CB peaks, in the so-called CB valleys, the dominating tunneling process is called co-tunneling, which is an elastic or inelastic tunneling via virtual intermediate states [9–12], that is responsible for the Kondo effect in the Fermi liquid, however in this Letter we will focus on sequential tunneling, since we are mostly interested in the modulation of the CB peaks. The sequential tunneling results from the sequence of three events: $A = \{\text{one electron tunnels from the left FQH liquid through the left QPC to the island}\}$, $B = \{\text{an electron could be accommodated at (and therefore transported along) the edge of the CB island}\}$ and $C = \{\text{an electron tunnels through the right QPC to the right FQH liquid}\}$. According to the Landauer formula the conductance $G_{\text{CB}} = (e^2/h)P(A \cap B \cap C)$ of the Fabry–Perot interferometer in the CB blockade regime is proportional to the three-event joint probability which is a product $P(A \cap B \cap C) = P(A \cap C)P(B)$ because B is statistically independent of A and C . Furthermore, the joint probability $P(A \cap C) = (h/e^2)G_{LR}$ is simply proportional to the conductance of two resistors in series $(G_{LR})^{-1} = G_L^{-1} + G_R^{-1}$, where G_L and G_R are the conductances of the left and right quantum point contact. Therefore the CB conductance is

$$G_{\text{CB}} = \frac{g_L g_R}{g_L + g_R} G_{\text{is}}, \quad g_{L,R} = \frac{h}{e^2} G_{L,R}, \quad (1)$$

with G_{is} being the conductance of the island’s edge. The conductances $G_{L,R}$ are independent of the area of the island and at low voltage depend on the temperature as $G_{L,R} \propto T^{4\Delta-2}$, where Δ is the scaling dimension of the electron.

The conductance G_{is} could be computed at zero temperature as the derivative of the persistent current, i.e., as a second derivative of the ground state energy, with respect to the Aharonov–Bohm (AB) flux ϕ using Kohn’s relation [13, 14]

$$\lim_{\omega \rightarrow 0} \omega \text{Im} \sigma(\omega) = -\frac{e^2 L^2}{\text{Vol} \hbar^2} \frac{\partial^2 E_0}{\partial \phi^2}. \quad (2)$$

This remarkable relation can be generalized for non-zero temperatures: the conductivity of the edge channel can be written in terms of the charge stiffness (related to the isothermal compressibility) due to the Einstein relation (see e.g., Eq. (2.81) in [15]),

$$\sigma(0) = e^2 D \left. \frac{\partial n}{\partial \mu} \right|_T, \quad (3)$$

where μ is the chemical potential, D is the diffusion coefficient and the thermodynamic derivative is taken at constant temperature. The Einstein relation (3) is proven by the standard Kubo linear response techniques [15].

In this Letter we will use the CFT [16] for the FQH edge [17, 18] to define the partition function for the edge and compute the thermodynamic derivative in (3).

The standard grand-canonical partition function for a FQH disk [19], [16], [7, 8, 20] could be written in terms of the Boltzmann factor $q = e^{2\pi i \tau} = e^{-\Delta \epsilon / k_B T}$, where the non-interacting energy spacing the edge is $\Delta \epsilon = \hbar 2\pi v_F / L$, as

$$Z_{\text{disk}}(\tau, \zeta) = \text{tr}_{\mathcal{H}_{\text{edge}}} e^{2\pi i \tau (L_0 - c/24)} e^{2\pi i \zeta J_0}, \quad (4)$$

where v_F is the Fermi velocity of the edge, L is the edge circumference, $H = \hbar \frac{2\pi v_F}{L} (L_0 - \frac{c}{24})$ is the edge Hamiltonian expressed in terms of the zero mode L_0 of the Virasoro stress-energy tensor, c is the central charge of the Virasoro algebra, $J_0 = N$ is the zero mode of the electric $u(1)$ current [21], which is equal to the Luttinger-liquid particle number operator. The Hilbert space $\mathcal{H}_{\text{edge}}$, over which the trace in (4) is taken, corresponds to a single FQH edge, i.e., the edge of the island which might contain non-trivial quasiparticles in the bulk. The two *modular* parameters [16], τ and ζ , are purely imaginary and are related to the temperature T and chemical potential μ as follows [21]

$$\tau = i\pi \frac{T_0}{T}, \quad T_0 = \frac{\hbar v_F}{\pi k_B L}, \quad \zeta = \frac{-i}{2\pi k_B T} \mu. \quad (5)$$

It is worth mentioning that the CFT partition functions are explicitly known for all FQH universality classes. The FQH disk is threaded by homogeneous perpendicular magnetic field, however, because the dynamics of the FQH liquid is concentrated at the edge, all thermodynamic quantities depend only on the product of the magnetic field and the area of the FQH disk, which could be varied by changing the voltage of the side gate [4]. The CFT partition function (4) in presence AB flux is modified by the flux-threading transformation [21]

$$\zeta \rightarrow \zeta + \phi \tau, \quad Z_{\text{disk}}^\phi(\tau, \zeta) = Z_{\text{disk}}(\tau, \zeta + \phi \tau), \quad (6)$$

and is different from the area-variation proposal of Ref. [8]. The physical interpretation of (6) will be discussed after Eq. (13) below. Because of this relation between the modular parameters ζ , τ and the AB flux ϕ , we will see below that the charge stiffness could be expressed as the second derivative of the grand potential of the edge with respect to the AB flux.

In order to compute the particle number average and its derivative with respect to the chemical potential we use Eq. (5) and the standard thermodynamic identification [19] of the grand potential on the edge $\Omega(T, \mu) = -k_B T \ln Z_{\text{disk}}(\tau, \zeta)$,

$$\langle n \rangle_{\beta, \mu} = -\frac{k_B T}{L} \frac{\partial}{\partial \mu} \ln Z_{\text{disk}}(\tau, \zeta) = \frac{1}{L} \langle J_0 \rangle_{\beta, \mu}, \quad (7)$$

where $\beta = (k_B T)^{-1}$ and the thermal average of A is

$$\langle A \rangle_{\beta, \mu} = Z_{\text{disk}}^{-1}(\tau, \zeta) \text{tr}_{\mathcal{H}_{\text{edge}}} A e^{2\pi i \tau (L_0 - c/24)} e^{2\pi i \zeta J_0}. \quad (8)$$

Next, in order to apply the Einstein relation (3) for G_{is} , we differentiate the particle density (7) with respect to μ

obtaining

$$\left\langle \frac{\partial n}{\partial \mu} \right\rangle_{\beta, \mu} = \frac{1}{Lk_B T} (\langle J_0^2 \rangle_{\beta, \mu} - \langle J_0 \rangle_{\beta, \mu}^2). \quad (9)$$

The grand potential $\Omega(T, \mu)$ depends on the AB flux ϕ because of (5) and (6). Computing the second derivative $\partial^2 \Omega / \partial \phi^2 = -(h\nu_F/L)^2 (\langle J_0^2 \rangle - \langle J_0 \rangle^2) / k_B T$ and comparing with (9) we obtain the main result in this Letter that the conductance $G_{\text{is}} = \sigma_{\text{is}}(0)/L$ of the edge is simply proportional (within Kubo's linear response theory) to the differential magnetic susceptibility $\kappa(T, \phi) = (e/h)\partial I(T, \phi)/\partial \phi$, where $I(T, \phi) = -(e/h)\partial \Omega(T, \phi)/\partial \phi$ is the persistent current (or, the orbital magnetization) on the edge, i.e.,

$$G_{\text{is}} = \frac{D}{v_F^2} \kappa(T, \phi), \quad \kappa = - \left(\frac{e}{h} \right)^2 \frac{\partial^2 \Omega(T, \phi)}{\partial \phi^2}. \quad (10)$$

As we will see below, the CB peaks of the DC conductance G_{is} correspond precisely to the paramagnetic peaks of the differential magnetic susceptibility $\kappa(\phi)$. The ‘‘diffusion’’ coefficient D for our one-dimensional ballistic channel of length $L/2$ is temperature independent and can be expressed in terms of the time of flight $\tau_f = L/(2v_F)$ as $D = v_F^2 \tau_f = v_F L/2$, see Sect. III.2 in [22].

The disk CFT partition function corresponding to a FQH droplet with filling factor $\nu_H = n_H/d_H$ can be written in general as a sum of products of Luttinger-liquid partition functions, with interaction parameter $g = n_H d_H$, representing the $u(1)$ charge, and neutral partition functions $\text{ch}_{\Lambda'}(\tau)$ [21]

$$Z_{\Lambda}^l(\tau, \zeta) = \sum_{s=0}^{n_H-1} K_{l+sd_H}(\tau, n_H \zeta; n_H d_H) \text{ch}_{\omega^s * \Lambda}(\tau), \quad (11)$$

where l (an integer defined mod d_H) and Λ denote respectively the $u(1)$ charge and neutral topological charge of the bulk quasiparticles, ω is the neutral topological charge of the electron operator [21], $*$ represents the fusion of two neutral topological charges and $\omega^s = \omega \cdots \omega$ is the s -fold fusion product [16]. In most cases the neutral topological charge Λ possesses a discrete \mathbb{Z}_{n_H} quantum number $P(\Lambda)$ and satisfies the *pairing rule* $P(\Lambda) \equiv l \pmod{n_H}$. The chiral Luttinger liquid grand canonical partition functions are explicitly [21]

$$K_l(\tau, \zeta; m) = \frac{\text{CZ}}{\eta(\tau)} \sum_{n=-\infty}^{\infty} q^{\frac{m}{2}(n+\frac{l}{m})^2} e^{2\pi i \zeta(n+\frac{l}{m})}, \quad (12)$$

where $\eta(\tau) = q^{1/24} \prod_{n=1}^{\infty} (1-q^n)$ and the non-holomorphic factor $\text{CZ} = \exp(-\pi \nu_H (\text{Im} \zeta)^2 / \text{Im} \tau)$ is known as the Cappelli–Zemba factor [20]. Because the statistics of the electron operator $\theta/\pi = 2\Delta = 1/\nu_H + \theta(\omega)$ must be an odd integer its neutral topological charge ω is always non-trivial when $n_H > 1$ and so are the neutral characters $\text{ch}_{\Lambda'}(\tau)$. For example, the neutral component of the electron for the \mathbb{Z}_3 Read–Rezayi (RR) FQH state [23] with

$\nu_H = 12/5$ is the parafermion field ψ_1 with $\Delta(\omega) = 2/3$ [24]. Although the neutral partition $\text{ch}_{\Lambda'}(\tau)$ are independent of ζ they do change the flux periodicity of the conductance peaks because of their contributions to the electron energies. For the numerical calculations below we use the following property [24]

$$K_l(\tau, n_H(\zeta + \phi\tau); n_H d_H) = K_{l+n_H \phi}(\tau, n_H \zeta; n_H d_H) \quad (13)$$

and set $\zeta = 0$. Since the electric charges of the excitations are given by the numbers multiplying $2\pi i \zeta$ in (11) and (12) it is easy to see that the number of electrons, corresponding to excitations with quantum numbers n and l (the same as in (12) for $m = n_H d_H$), in the right-hand-side of (13) is $N = n_H n + l/d_H + \nu_H \phi$ so that the addition of AB flux ϕ , according to (6), changes the number of electrons by $\nu_H \phi$ as it should be in order for the universal quantum Hall charge–flux relation (see Eq. (3) in [21]) to hold. This gives the physical interpretation of the flux-threading transformation (6). It also follows from (13), (6), (11) and (12) that the flux period is at most $\Delta\phi = d_H$ for any FQH state, because of the index-periodicity of the K functions: $K_{l+n_H d_H}(\tau, n_H \zeta; n_H d_H) = K_l(\tau, n_H \zeta; n_H d_H)$.

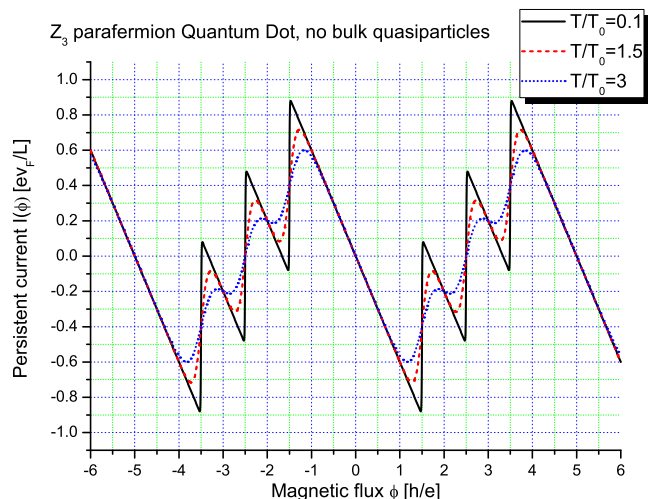


Fig. 2: (color online) Persistent current for a CB island which is in the \mathbb{Z}_3 parafermion FQH state without bulk quasiparticles.

We consider the case without bulk-edge relaxation which means that the electron arriving at the edge of the CB island moves fast enough from the left QPC to the right one without being able to fuse with bulk quasiparticles. Under the assumption that the velocities of the charged and neutral modes are the same we plot in Fig. 2 the persistent current $I(T, \phi)$, as a function of the AB flux, for the \mathbb{Z}_3 RR state corresponding to $n_H = 3$, $d_H = 5$ and the neutral partition functions, $\text{ch}_0 \equiv \text{Ch}_{00}$, $\text{ch}_\omega \equiv \text{Ch}_{01}$, $\text{ch}_{\omega^2} \equiv \text{Ch}_{02}$ corresponding to $l = 0$, $\Lambda = 0$ in (11) (i.e., no bulk quasiparticles), have been taken from Eq. (4.14) in [24]. If the velocities are different then the flux periods can be calculated in a similar way. We see from Fig. 2 that the tunneling of a single electron into the edge of

the CB island corresponds to a jump, of universal size approaching $e\nu_F/L$ at zero temperature, in the persistent current and that $\Delta\phi = 5$. The corresponding peaks of

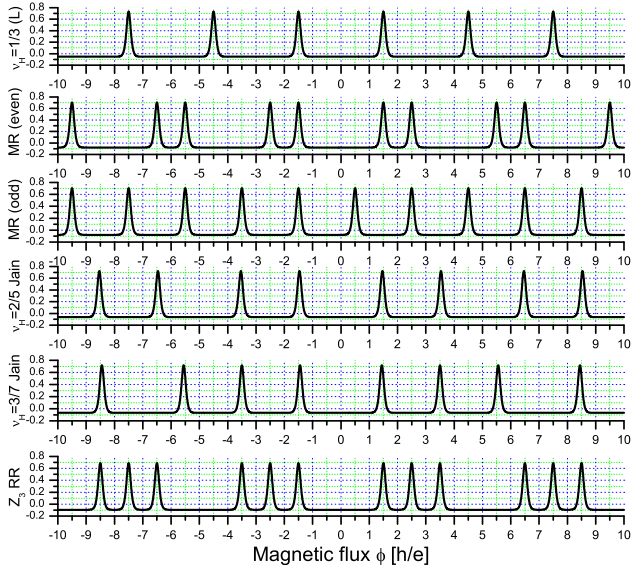


Fig. 3: Differential magnetic susceptibility $\kappa(\phi)$, at temperature $T/T_0 = 1$, in units $\frac{e^2}{h} \frac{2\pi\nu_F}{L}$ for various FQH states with no bulk quasiparticles, except for the third plot—MR (odd)—which is of the MR state with a single bulk quasiparticle.

the differential magnetic susceptibility are shown in the last plot of Fig. 3, from which we see that the peaks are clustered in triples separated by $\Delta\phi_1 = 1$ inside of the cluster and by $\Delta\phi_2 = 3$ between the clusters. The other plots in Fig. 3 are constructed from the following partition functions (11): $\nu_H = 1/3$ (L) is the Laughlin state ($n_H = 1$, $d_H = 3$, no neutral partition functions); MR (even) is the Moore–Read (MR) FQH state [25], $n_H = 2$, $d_H = 4$ with neutral partition functions, for $l = 0$, $\Lambda = 0$ in (11), ch_0 and $\text{ch}_\omega = \text{ch}_{1/2}$ taken from Eq. (7) in [26]; MR (odd) is the MR state with one quasiparticle in the bulk and for $l = 1$, $\Lambda = \sigma$, where σ is the Ising anyon, with neutral partition functions $\text{ch}_\Lambda = \text{ch}_{\omega*\Lambda} = \text{ch}_{1/16}$ taken from Eq. (7) in [26]—this CB peaks pattern is identical with that for the $g = 1/2$ Luttinger liquid—this change of the total flux period from 4 to 2 is the even–odd effect in the MR state [3]; the fourth plot corresponds to the hierarchical $\nu_H = 2/5$ Jain FQH state with $n_H = 2$, $d_H = 5$ and neutral partition functions, for $l = \Lambda = 0$, $\text{ch}_0 = K_0(\tau, 0; 2)$ and $\text{ch}_\omega = K_1(\tau, 0; 2)$; the fifth plot is of the $\nu_H = 3/7$ Jain state, which corresponds to $n_H = 3$, $d_H = 7$ in Eq. (11) with $l = \Lambda = 0$ and neutral partition functions $\text{ch}_0 = \text{ch}_{(0,0)}$, $\text{ch}_\omega = \text{ch}_{(1,0)}$ and $\text{ch}_{\omega^2} = \text{ch}_{(0,1)}$ taken as the characters [16] of the vacuum and fundamental representations of the current algebra $\widehat{su(3)}_1$. The flux spacing of the peaks in Fig. 3 are in perfect agreement with those of the CB peaks obtained earlier in the literature for zero temperature [3–8] by analyzing the flux dependence of the electron energies at the CB resonances. However,

our results also allow us to estimate the shape, height and width of the CB peaks at finite temperature, which is important for the experiments. One interesting feature of the

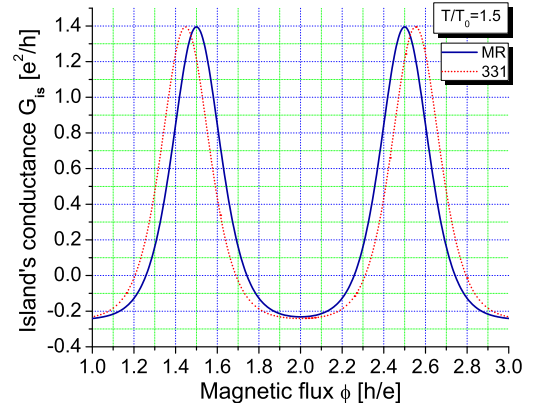


Fig. 4: (color online) Island’s conductance for the Moore–Read and 331 FQH states (without bulk quasiparticles).

CB peaks, which demonstrates the advantage of the CFT approach, is that they may become displaced at finite T , in states such as the 331, $\nu_H = 2/5$ and $\nu_H = 3/7$ Jain states, due to electron multiplicities in the neutral sector. Consider, e.g., the 331 (Halperin) FQH state, which corresponds to $n_H = 2$, $d_H = 4$ and neutral partition functions $\text{ch}_0 = K_0(\tau, 0; 4)$ and $\text{ch}_\omega = K_2(\tau, 0; 4)$. It has been demonstrated earlier that the CB peaks patterns of the 331 and MR state are indistinguishable at $T = 0$ and the situation is similar for other FQH states with different topological orders [6]. When the temperature increases, the CB peaks in the 331 state are displaced in such a way that the short period $\Delta\phi_1 = 1$ increases (by approximately 0.1 h/e in Fig. 4), while the long one $\Delta\phi_2 = 3$ decreases keeping the total periodicity $\Delta\phi = 4$ unchanged. This can be explained as follows—due to neutral multiplicities, $m = 2$ in this case, the neutral character of the electron sector (without bulk quasiparticles), for $T \ll T_0$, is $\text{ch}_\omega(\tau) \simeq m q^{\Delta_0} = q^{\Delta'_0}$ where Δ_0 is the neutral CFT dimension of the electron and

$$\Delta'_0 = \Delta_0 - \frac{1}{2\pi^2} \frac{T}{T_0} \ln m. \quad (14)$$

Thus, increasing T effectively lowers the neutral energy of the electron and therefore displaces the CB peaks, which appear at flux positions at which two parabolas, shifted in the vertical direction by the neutral electron energy, cross (see e.g., Fig. 3 in [8]). We see from our Fig. 4, that the finite-temperature CB peak patterns of the MR and 331 states are not identical and this temperature dependence of the CB peak’s periods could in principle be used to distinguish between them.

Similar asymmetry and displacement of the CB peaks could be seen in the $\nu = 2/5$ Jain state, where the neutral electron multiplicity is $m = 2$ again [8], see Fig. 5. The distances between the peaks are $\Delta\phi_1 = 2$, $\Delta\phi_2 = 3$ giving

total periodicity $\Delta\phi = 5$. When temperature increases the short period $\Delta\phi_1$ tends to increase while $\Delta\phi_2$ decreases keeping the total periodicity the same. Also, in the $\nu_H =$

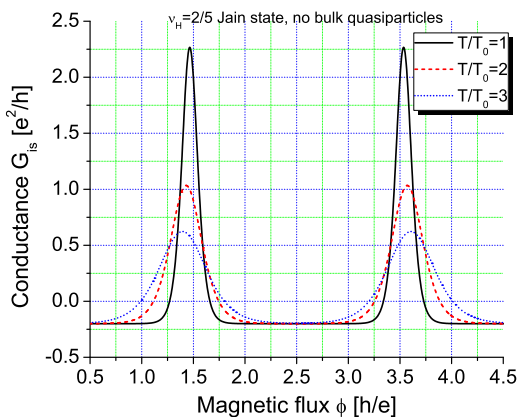


Fig. 5: (color online) Peak asymmetry for the $\nu = 2/5$ Jain FQH state due to the neutral-sector multiplicities. This picture is reproduced periodically along the ϕ axis with period $\Delta\phi = 5$.

$3/7$ Jain FQH state the tendency is again for the short period $\Delta\phi_1 = 2$ to increase, while the long period $\Delta\phi_2 = 3$ to decrease when increasing the temperature, and this is again attributed to the neutral multiplicities [8].

For the \mathbb{Z}_3 RR state the positions of the peaks and the distances between them do not change with temperature, but the peaks decrease and broaden, see Fig. 6. Eq. (11) allows us to derive an analytical estimate of the

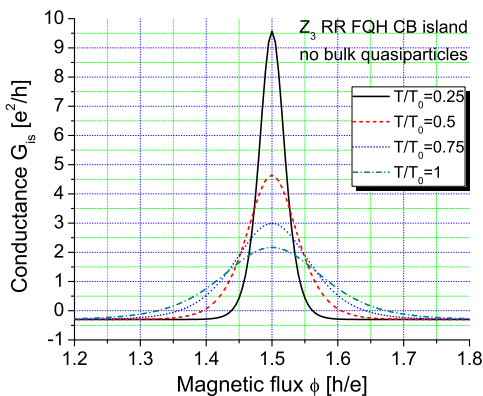


Fig. 6: (color online) Broadening of the CB peaks in the \mathbb{Z}_3 parafermion (RR) FQH droplet without bulk quasiparticles.

height, width and shape of the CB peaks at low temperature. Keeping only the leading terms in (11) for $q = \exp(-\Delta\epsilon/k_B T) \rightarrow 0$, which for $l = \Lambda = 0$ are the terms with $s = 0, \pm 1 \pmod{n_H}$ in (11) and $n = 0$ in (12), it can be shown that the partition function (11) has the following low-temperature approximation (no bulk quasiparticles) for $|\phi - \Delta| < 1/2$

$$Z(T, \phi) \underset{T \ll T_0}{\approx} q^{\nu_H \frac{\phi^2}{2}} \left[1 + 2q^\Delta \cosh\left(\frac{\Delta\epsilon}{k_B T} \phi\right) \right], \quad (15)$$

where $\Delta = 1/(2\nu_H) + \Delta_0$ is the total CFT dimension of the electron. Then the CB conductance (1) for the case without neutral multiplicities has a universal peak shape given by

$$G_{CB} \underset{T \ll T_0}{\approx} \frac{g_L g_R}{g_L + g_R} \frac{e^2}{h} \left(-\frac{1}{2}\right) \frac{\partial}{\partial \phi} \left(\frac{1}{1 + e^{\frac{\Delta\epsilon}{k_B T}(\phi - \Delta)}} \right) \quad (16)$$

and therefore the peak's height can be estimated to be

$$G_{CB}^{\text{peak}} \underset{T \ll T_0}{\approx} \frac{g_L g_R}{g_L + g_R} \frac{e^2}{h} \frac{\Delta\epsilon}{8k_B T}, \quad (17)$$

which is consistent with previous estimates (see Eqs. (24) in [22], Eq. (134) in [27] and Eq. (1) in [9]). Notice that (17) has crucial implications for the experimental observability of the CB peaks at low temperatures. The dimensionless tunneling conductances $g_{L,R}$ for the left and right QPC's, defined in (1), which appear in Eq. (17) depend on temperature [9] as $g_{L,R} \propto T^{2\Delta_{L,R} + 2\Delta_{QD} - 2} = T^{4\Delta - 2}$, where $\Delta_{L,R}$ is the CFT dimension of the electron in the Left, Right lead, while Δ_{QD} is the CFT dimension on the quantum dot and we have chosen $\Delta_L = \Delta_R = \Delta_{QD} = \Delta$. According to (17) the island conductance's peak is $G_{is} \propto T^{-1}$ and therefore the total CB conductance vanishes at zero temperature

$$G_{CB}^{\text{peak}} \propto T^{4\Delta - 3}, \quad T \ll T_0 \quad (18)$$

for most FQH liquids since the electron dimension (which must be half-integer) is $\Delta \geq 3/2$. The coefficient of proportionality depends on the bare tunneling amplitudes of the left and right QPC's which do not renormalize because the electron tunneling is irrelevant in the sense of the RG flow and therefore the strong-reflection regime of the Fabry–Perot interferometer, shown in Fig. 1, is a stable RG fixed point. Notice that the conductance scaling with temperature, which we use here corresponds to Sect. IV in Ref. [9] and has to be distinguished from the results of Sect. III there, where the quantum dot contribution has not been taken into account correctly.

Substituting (14) in (15) for the 331 and $\nu_H = 2/5$ Jain states we obtain that the short flux period increases as a function of the temperature as

$$\Delta\phi_1(T) = \Delta\phi_1(0) + \frac{1}{\pi^2} \frac{T}{T_0} \ln m, \quad (19)$$

where the neutral electron multiplicity is $m = 2$.

As can be seen from Eq. 16 and Figs. 4, 5 and 6, the (sequential-tunneling) conductance decreases exponentially away from the CB peak's centers and becomes negative in the CB valleys, however, the co-tunneling conductance decays only algebraically [9], hence is the main transport mechanism in the CB valleys, and the total conductance remains positive.

If we define the width $\delta\phi = |\phi_2 - \phi_1|$ of a CB peak as the difference between the two flux positions ϕ_1 and ϕ_2 ,

around the peak, at which $G_{\text{is}}(\phi_{1,2}) = 0$, resp., $\kappa(\phi_{1,2}) = 0$, then using (15) we can prove that the peaks' width is not simply proportional to the temperature—instead, there is a logarithmic correction

$$\delta\phi(T) \underset{T < 3T_0}{\simeq} \frac{1}{\pi^2} \left(\frac{T}{T_0} \right) \left[\ln \left(\frac{2\pi^2}{\nu_H} \right) - \ln \left(\frac{T}{T_0} \right) \right]. \quad (20)$$

However, as we discussed above, when the conductance begins to decrease, due to deviation of the flux from the CB peak's center, there is a crossover to co-tunneling regime. Therefore we could define the CB peak's width at level σ , such that the conductance at the points $\phi_{1,2}$ defining the width is $G_{\text{CB}}(\phi_{1,2}) = \sigma G_{\text{CB}}^{\text{peak}}$, where sequential tunneling is still the dominating process. Then, ignoring a logarithmic term similar to that in (20), we find that the width of the CB peak at level σ increases linearly with temperature

$$\begin{aligned} \delta\phi(T)|_{\sigma} &= \frac{\alpha}{2\pi^2} \left(\frac{T}{T_0} \right), \quad \text{where } \frac{1}{2} \leq \sigma < 1 \text{ and} \\ \alpha &= -2 \ln \left[\left(\frac{2}{\sigma} - 1 \right) - \sqrt{\left(\frac{2}{\sigma} - 1 \right)^2 - 1} \right]. \end{aligned}$$

Notice that this estimate of the CB peak's width is independent of the filling factor ν_H because it is derived from Eq. (16) which is universal and independent of ν_H .

In conclusion, we showed that the CB conductance peaks, for a Fabry–Perot interferometer realized in a FQH bar, could be computed at finite temperature in terms of the differential magnetic susceptibility derived within the equilibrium effective CFT for the FQH edge states. Using the known chiral partition functions for a number of FQH states we derived the positions of the CB peaks, their spacing, universal shape, height and width. While the CB peak spacing coincides with previous results in the literature, the new estimates for the peak's height and width at finite temperature could give important hints about the experimental observation of the CB. In addition, the asymmetry and displacement of the CB peaks positions at finite temperature could give important information about the neutral multiplicities in the corresponding FQH states, eventually providing signatures to distinguish different FQH states with similar zero-temperature CB patterns.

Acknowledgments: I am grateful to Reinhold Egger for useful discussions. The author has been supported by the Alexander von Humboldt Foundation. This work has been partially supported by the BG-NSF under Contract No. DO 02-257.

REFERENCES

- [1] ZHANG Y., MCCLURE D. T., LEVENSON-FALK E. M., MARCUS C. M., PFEIFFER L. N. and WEST K. W., *Phys. Rev. B*, **79** (2009) 241304(R).
- [2] BISHARA W., BONDERSON P., NAYAK C., SHTENDEL K. and SLINGERLAND J. K., *Phys. Rev. B*, **80** (2009) 155303.
- [3] STERN A. and HALPERIN B. I., *Phys. Rev. Lett.*, **96** (2006) 016802.
- [4] ILAN R., GROSFELD E. and STERN A., *Phys. Rev. Lett.*, **100** (2008) 086803.
- [5] ILAN R., GROSFELD E., SCHOUTENS K. and STERN A., *Phys. Rev. B*, **79** (2009) 245305.
- [6] BONDERSON P., NAYAK C. and SHTENDEL K., *Phys. Rev. B*, **81** (2010) 165308.
- [7] CAPPELLI A., GEORGIEV L. S. and ZEMBA G. R., *J. Phys. A: Math. Theor.*, **42** (2009) 222001.
- [8] CAPPELLI A., VIOLA G. and ZEMBA G. R., *Annals of Physics*, **325** (2010) 465.
- [9] FURUSAKI A., *Phys. Rev. B*, **57** (1998) 7141.
- [10] AVERIN D. V. and NAZAROV Y. V., *Phys. Rev. Lett.*, **65** (1990) 2446.
- [11] HEINZEL T., MANUS S., WHARAM D. A., KOTTHAUS J. P., BÖHM G., KLEIN W., TRÄNKLE G. and WEIMANN G., *Europhys. Lett.*, **26** (1994) 685.
- [12] WEYMANN I., *Europhys. Lett.*, **76** (2006) 1200.
- [13] KOHN W., *Phys. Rev.*, **133** (1964) A171.
- [14] IMRY Y., *Introduction to mesoscopic physics* (Oxford University Press) 1997.
- [15] DI VENTRA M., *Electrical transport in nanoscale systems* (Cambridge University Press) 2008.
- [16] DI FRANCESCO P., MATHIEU P. and SÉNÉCHAL D., *Conformal Field Theory* (Springer-Verlag, New York) 1997.
- [17] WEN X.-G., *Int. J. Mod. Phys. B*, **4** (1990) 239.
- [18] FROELICH J. and ZEE A., *Nucl. Phys. B*, **364** (1990) 517.
- [19] KUBO R., TODA M. and HASHITSUME N., *Statistical Physics II* (Springer-Verlag, Berlin) 1985.
- [20] CAPPELLI A. and ZEMBA G. R., *Nucl. Phys. B*, **490** (1997) 595.
- [21] GEORGIEV L. S., *Nucl. Phys. B*, **707** (2005) 347.
- [22] ALHASSID Y., *Rev. Mod. Phys.*, **72** (2000) 895.
- [23] READ N. and REZAYI E., *Phys. Rev. B*, **59** (1998) 8084.
- [24] CAPPELLI A., GEORGIEV L. S. and TODOROV I. T., *Nucl. Phys. B*, **599** [FS] (2001) 499.
- [25] MOORE G. and READ N., *Nucl. Phys. B*, **360** (1991) 362.
- [26] GEORGIEV L. S., *Nucl. Phys. B*, **651** (2003) 331.
- [27] ALEINER I., BROUWER P. and GLAZMAN L., *Phys. Rep.*, **358** (2002) 309.